AIAA–2002–0569
Noise, Turbulence, and Thrust of Subsonic Free Jets From Lobed Nozzles

K.B.M.Q. Zaman and F.Y. Wang
NASA Glenn Research Center
Cleveland, OH

40th AIAA Aerospace Sciences Meeting & Exhibit
January 14–17, 2002 / Reno, NV

AIAA–2002–0569

NOISE, TURBULENCE, AND THRUST OF SUBSONIC FREE JETS FROM LOBED NOZZLES

K.B.M.Q. Zaman* and F.Y. Wang†
National Aeronautics and Space Administration
Glenn Research Center
Cleveland, Ohio 44135

ABSTRACT

A study of noise benefit, vis-à-vis thrust penalty, and its correlation to turbulence intensities was conducted for free jets issuing from lobed nozzles. Four convergent nozzles with constant exit area were used in the experiments. Three of these were of rectangular lobed configuration having six, ten and fourteen lobes; the fourth was a circular nozzle. Increasing the number of lobes resulted in a progressive reduction in the turbulence intensities as well as in the overall radiated noise. The noise reduction was pronounced at the low frequency end of the spectrum. However, there was an increase in the high frequency noise that rendered the overall benefit less attractive when compared on a scaled-up A-weighted basis. A reduction in noise was accompanied by a commensurate reduction in the turbulent kinetic energy in the flow field. As expected, increasing the number of lobes involved progressive reduction in the thrust coefficient. Among the cases studied, the six-lobed nozzle had the optimum reduction in turbulence and noise with the least thrust penalty.

INTRODUCTION

This experimental investigation was prompted by an earlier study[1] in which far-field noise of high subsonic jets from rectangular, tabbed and lobed nozzles were reported. A six-lobed nozzle exhibited significantly lower noise compared to the other cases. Later, through limited experiments, the lobed nozzle was also found to involve remarkably lower turbulence intensities.[2,3] A detailed study of the noise benefit, the corresponding thrust penalty, and its correlation to the structure of the turbulent flow field was considered a worthy effort. This led to the present investigation.

'Lobed forced mixers' or corrugated splitter plates are often used in the Industry in order to achieve efficient mixing between two streams. There have been several studies of a basic two-stream mixing layer originating from such a splitter plate.[4–8] One obvious effect of the lobed geometry is the increase in the interfacial area between the two streams that enhances the mixing. Depending on the geometry, the lobes can also introduce pairs of counter-rotating streamwise vortices that efficiently transport momentum and species across the mixing layer. Cross-stream components of vorticity shed from the trailing edges of the lobes, and their subsequent dynamics, can also play a role in the mixing enhancement.

Many researchers have investigated jet flows from nozzles with lobed exit lips or other modified shapes.[9–15] Faster spreading of the jet was observed in all instances. Furthermore, some reduction in jet noise with the use of lobed nozzles has been observed in some of the cited work as well as in the Industry. Unfortunately, because of the complex geometry and large parameter-space the underlying flow mechanisms have remained far from being completely understood. The processes that impact the noise field of these nozzles are even less understood at this time. It is apparent that further model-scale experiments would be helpful for advancing the understanding and providing a database for developing engineering correlations for the prediction of mixing and noise. It is with this spirit the present investigation was initiated. The objective has been to measure the flow and noise fields in detail for a systematic parametric variation.

Because of the many parameters, only limited variation was possible. The goal was set to examine the effect of the number of lobes for a fixed exit area of the nozzle. The nozzles were convergent and the experiments involved 'cold', free jets. Most of the data were

* Aerospace Engineer, Turbomachinery and Propulsion Systems Division, Associate Fellow, AIAA.
† Presently with John A. Volpe Center, U.S. Department of Transportation, Cambridge, MA, Senior Member, AIAA.

taken at a high subsonic Mach number (0.94) to allow reliable noise measurement while avoiding shock-associated complications of supersonic flows. The flow surveys at that condition, on the other hand, had to be limited because of inherent measurement difficulty in compressible flows. Nevertheless, after demonstrating that the centerline velocity and turbulence profiles at the high (0.94) and low (0.30) Mach number were essentially similar, further flow field measurement was conducted at the latter condition. The field data, and some integrals obtained from them, were examined in order to assess the impact of the number of lobes. These results are summarized in the following.

EXPERIMENTAL PROCEDURE

The data were obtained in an open jet facility. Compressed air passed through a cylindrical plenum chamber fitted with flow conditioning units and then through the nozzle to discharge into the quiescent ambient. The experiments involved 'cold' flows, i.e., the jet was unheated and the total temperature was approximately the same throughout and equaled that in the ambient.

Data from four nozzles are to be presented. All have convergent interiors with approximately ¼ - inch long constant cross-section passage prior to the exit. The equivalent diameter (D) based on the exit area is 0.58 inch for all four cases. One of the four nozzles is of circular geometry serving as the 'baseline' case. The rest are of lobed configurations, having six, ten and fourteen lobes. The exit geometry (for the 10-lobed case) is shown schematically in Fig. 1 and the relevant dimensions for all cases are listed in table 1. The last column shows the ratio of hydraulic diameter (based on the perimeter) to equivalent diameter (based on the area), which is a measure of 'perimeter stretching' caused by the lobes.

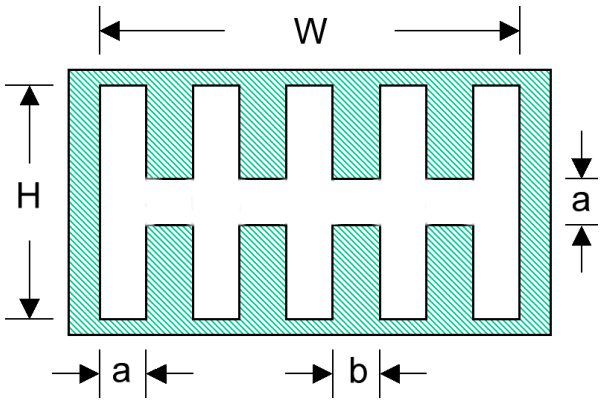

Figure 1. Schematic of exit geometry of 10-lobed nozzle.

Table 1. Lobed nozzle geometry; dimensions are in inches.

Nozzle	W	H	a	b	D_h/D
6-lobe	1.253	0.825	0.2689	0.2230	3.501
10-lobe	1.253	0.825	0.1743	0.0953	5.137
14-lobe	1.253	0.825	0.1281	0.0593	6.870

Standard procedures were followed for far-field noise measurement using a ¼-inch microphone (B&K). The measurement location was 63D from the jet exit. Spectral analysis was done with a 400-line analyzer (Nicolet). Noise data were obtained at two angles (θ) relative to the jet axis. An orifice meter mounted on the supply line measured mass flow rate. Thrust was measured by a one-component force-balance; further details can be found in Ref. 16. Repeatability of the noise spectral amplitudes was within 0.5 dB. Uncertainty in the thrust data was within 1%.

As stated in the introduction, most of the data were obtained for a nominal jet Mach number of 0.94. At this Mach number, hot-wire data were obtained only on the jet axis due to probe breakage and other difficulties. However, detailed survey of the 3-dimensional flow field was conducted at a jet Mach number of 0.30. The measurement at the lower Mach number was unambiguous, free from sensor survivability problems, and inexpensive since the lower supply pressure could be furnished with an auxiliary blower. The independent operation with the blower allowed sustained runs over long periods that were necessary in the surveys. While the velocity and turbulence data at the lower Mach number represent the streamwise components, the data at the higher Mach number are only qualitative. A relatively high overheat ratio was used in the constant-temperature anemometer so that the hot-wire essentially responded to mass flux (velocity times density) in the latter condition. Limited data were obtained at the higher Mach number using particle image velocimetry (PIV); the procedure will be briefly described with the data.

RESULTS

Figure 2(a) shows sound pressure spectra, at $\theta = 90°$, for the three lobed cases compared to the baseline circular case. For these data the supply pressure is held constant; thus, the jet Mach number is the same for all cases. It is apparent that the noise is low for all lobed cases. Increasing the number of lobes from 6 to 10 produces some additional noise benefit. However, there is only marginal gain with further increase in the number of lobes to 14. Figure 2(b) shows spectra for the same cases of Fig. 2(a) except that the thrust is held constant (thrust for the 14-lobed nozzle is the same between the two figures). A similar conclusion is reached regarding the influence of number of lobes. However, it can be seen that the high-frequency noise for the 10 and

14-lobed cases are relatively high. The implication of this is discussed shortly. Corresponding noise spectra at $\theta = 25°$, for constant Mach number are shown in Fig. 3(a), and for constant thrust are shown in Fig. 3(b). Again, a similar observation can be made regarding the effect of number of lobes.

The spectra in Figs. 2 and 3 are obtained on the minor axis plane. Corresponding data obtained on the major axis plane are compared for the 6-lobed nozzle, as an example, in Fig. 4. At $\theta = 90°$ in (a), there is practically no difference in the spectra between the minor and the major axis planes. This demonstrates the axisymmetry of the noise field,[1] even though the flow field is quite asymmetric initially. At $\theta = 25°$, the amplitudes are identical at lower frequencies; however, high-frequency amplitudes are higher on the minor axis plane.

The overall sound pressure levels, obtained by integration of the spectral data of Figs. 2 and 3, are shown in Fig. 5(a). The data are shown as a function of number of lobes, with the circular jet data shown at an abscissa value of unity. The amplitudes decrease with increasing number of lobes, for both values of θ and for both cases

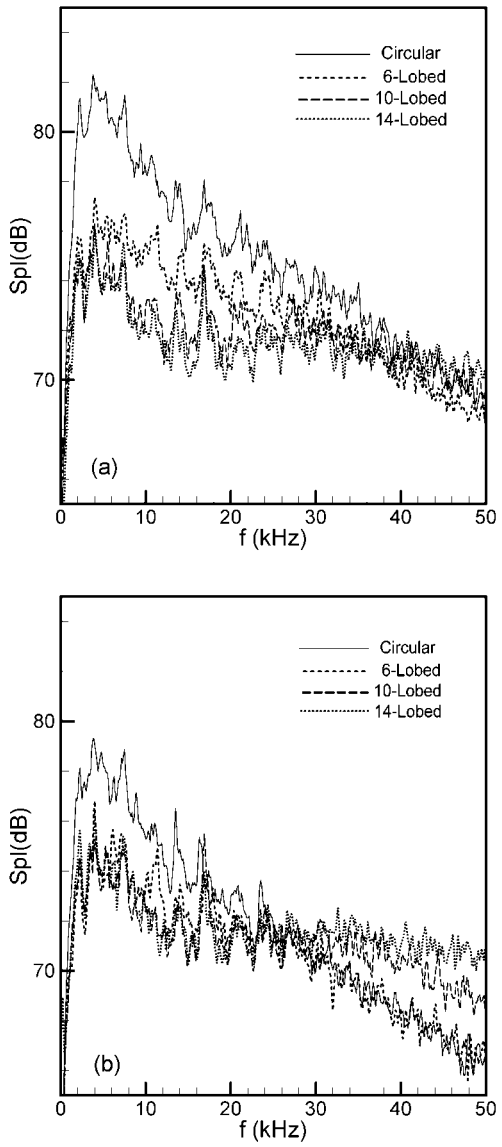

Figure 2. Sound pressure spectra at $\theta = 90°$, on minor axis, for indicated nozzles; (a) constant pressure ratio, $M_j = 0.94$, (b) constant thrust, $T \approx 17$ N.

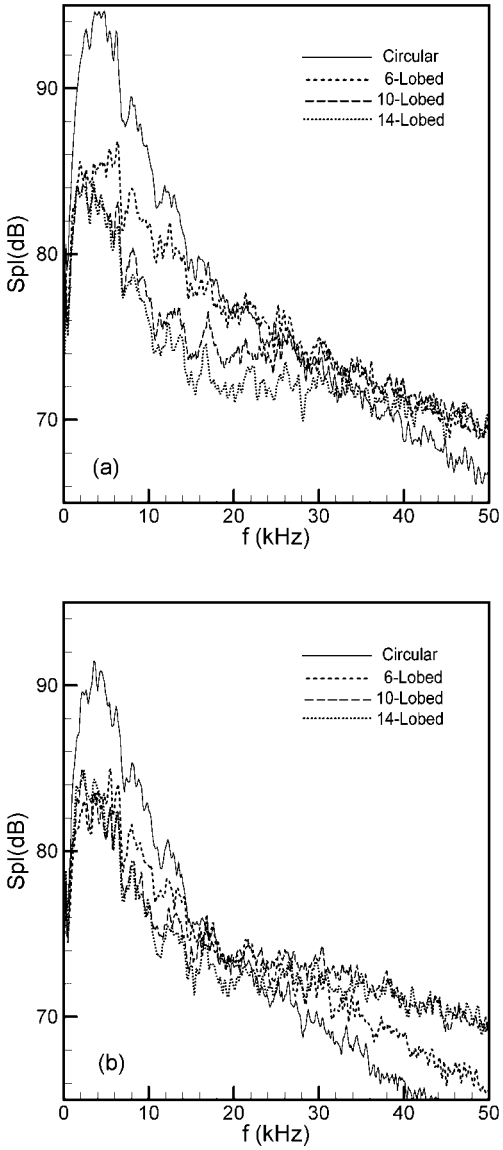

Figure 3. Sound pressure spectra at $\theta = 25°$, on minor axis, for indicated nozzles; (a) constant pressure ratio, $M_j = 0.94$, (b) constant thrust, $T \approx 17$ N.

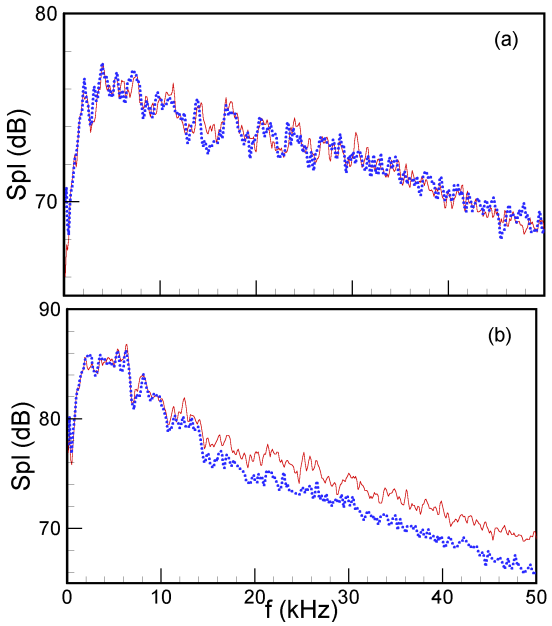

Figure 4. Sound pressure spectra for 6-lobed nozzle at M_j = 0.94; solid line: minor axis, dotted line: major axis. (a) θ = 90°, (b) θ = 25°.

of constant Mach number and constant thrust. However, the increased high-frequency noise can weigh in differently in 'perceived noise levels'. To assess this, A-weighted noise levels were calculated and shown in Fig. 5(b). The levels are somewhat different but the trend remains the same as seen in Fig. 5(a).

Furthermore, in order to simulate the noise from a realistic practical nozzle the spectra data were scaled by a factor of 20, i.e., assuming a 'Strouhal number scaling', the frequencies were divided by 20 to simulate noise from a 20 times larger nozzle. The data were then integrated to obtain the A-weighted (dBA) levels. The results are shown in Fig. 5(c). It is apparent that, after these considerations, the noise benefit is not as attractive as it first appeared. However, the applicability of Strouhal number scaling, invoked in Fig. 5(c), might be questionable especially at the high frequency end of the spectrum. Nevertheless, a net noise reduction with the six-lobed nozzle is evident for all conditions. Further reduction with more number of lobes appears marginal or questionable.

Thrust and mass flow rate data for the four nozzles are shown in Figs. 6 and 7, respectively, as a function of jet Mach number. The solid lines in these figures represent ideal values (assuming a top-hat exit velocity profile with zero boundary layer thickness). Data for the circular and 6-lobed cases are hardly distinguishable from the ideal curves. However, there is noticeable thrust loss and flow blockage for the 10- and 14-lobed nozzles.

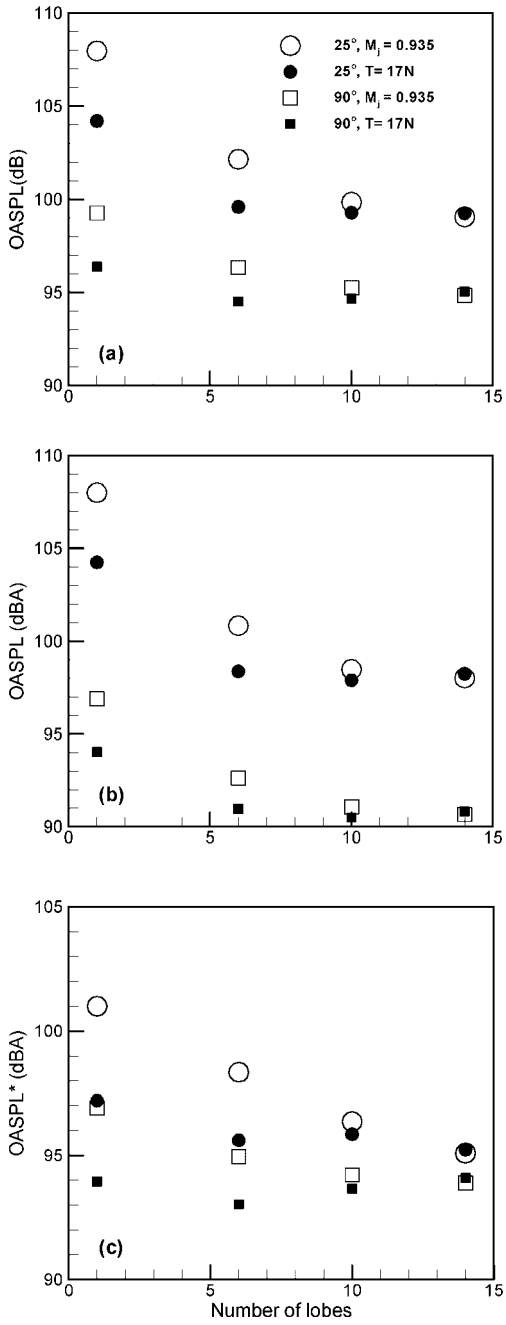

Figure 5. Overall sound pressure level corresponding to the data of Figs. 2 and 3, shown as a function of number of lobes. (a) OASPL, (b) A-weighted OASPL, (c) A-weighted OASPL after scaling by a factor of 20.

Thrust coefficient, calculated from the data of Figs. 6 and 7, are shown in Fig. 8. It is essentially unity, (within measurement uncertainty), for the circular nozzle. It is clearly but only slightly lower for the 6-lobed case. At M_j = 0.94, about 7 dBA noise reduction

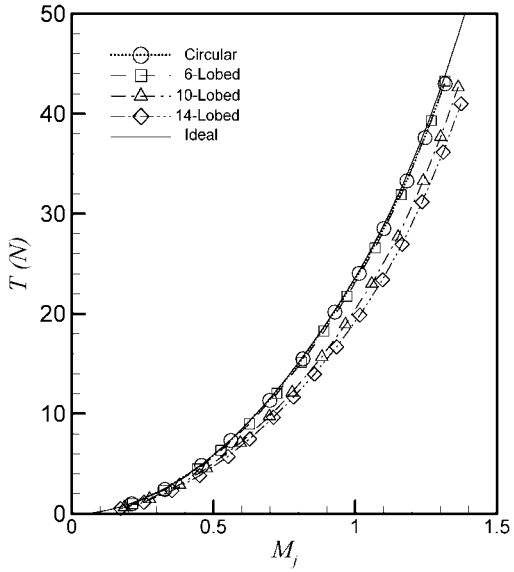

Figure 6. Thrust versus M_j for indicated nozzles.

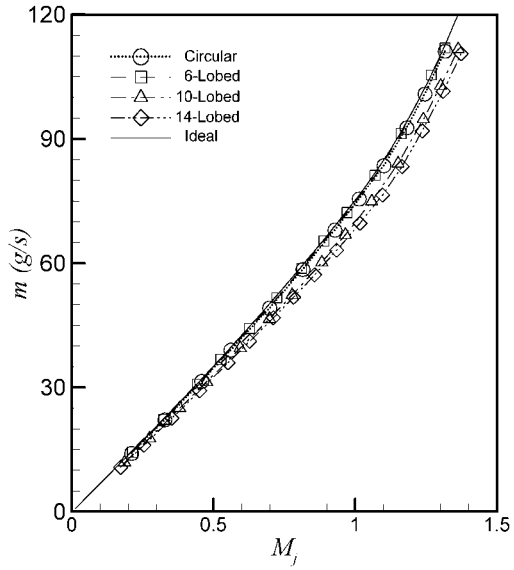

Figure 7. Mass flow rate versus M_j for indicated nozzles.

(Fig. 5(b); θ = 25° case) has been achieved while C_f dropped to 0.982. (For constant thrust the corresponding reduction is about 5 dBA.) With increasing number of lobes C_f becomes significantly lower than unity.

Centerline variations of 'mean velocity' and 'turbulence intensity' are shown in Figs. 9(a) and (b), for M_j = 0.94. As stated in §2, the hot-wire data are approximations of mass flux (ρu) rather than velocity (u). A faster decay of the mean value is observed for the lobed nozzles, indicating a faster jet spreading. Corresponding turbulence data (Fig. 9(b)) show that a peak occurs close to the nozzle, and that the location of this

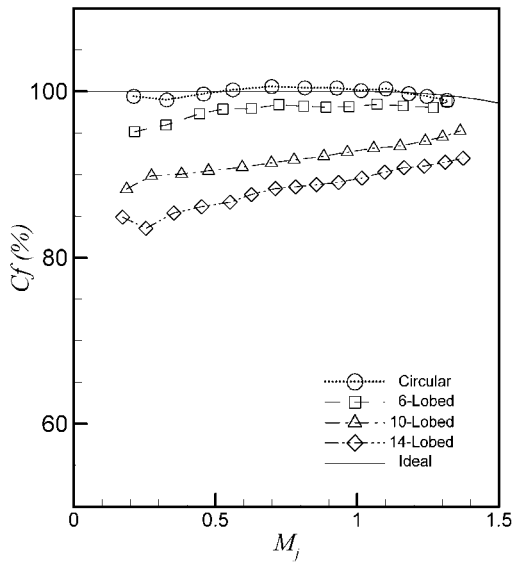

Figure 8. Thrust coefficient versus M_j for indicated nozzles.

peak shifts upstream with more number of lobes. There occurs a second peak in the range $8<x/D<10$. The second peak for any of the lobed cases is found to be of much smaller amplitude compared to the peak for the circular case. The lower turbulence, in the 'noise-producing region', is commensurate with the lower far-field noise for the lobed cases (Figs. 2–5).

Detailed flow field measurement at M_j = 0.94 was attempted using the PIV technique. A Thermo-systems Inc. (TSI) instrument package was used for the measurement. The flow in the plenum chamber was seeded with olive oil based fog particles. Mean and rms velocity fields were measured based on averages over 56 frames. An algorithm following Ref. 17 was adopted in the data reduction. However, due to drifts in seeding, laser system and alignment of optics good data repeatability could not be ensured. The results, considered qualitative, for only the circular and the 14-lobed nozzles are shown in Figs. 10 and 11.

The mean velocity fields for the two nozzles are compared in Fig. 10 while the turbulence intensity fields are compared in Fig. 11. The turbulence results confirm the occurrence of a high-intensity region close to the nozzle, observed earlier with the hot-wire data (Fig. 9(b)). The flow fields in Figs. 10 and 11 extend up to about x/D = 4.5. Thus, the second high intensity region of Fig. 9(b) is not captured. It should be apparent that the second peak, occurring on the jet axis, takes place following the merger of the outer shear layers. The occurrence of the first peak close to the nozzle is somewhat intriguing and this is further explored with hot-wire anemometry.

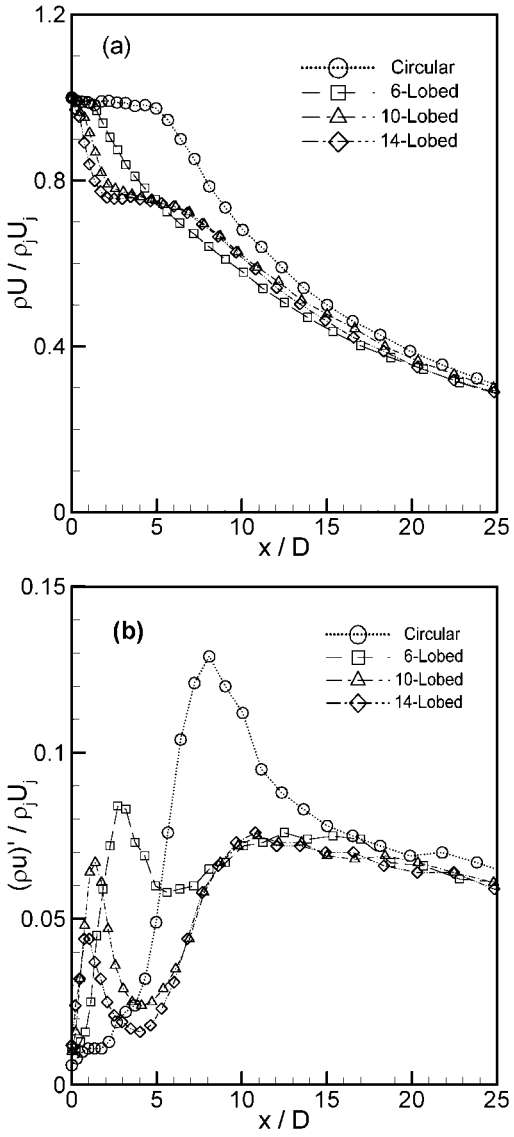

Figure 9. Hot-wire results for centerline profiles at $M_j = 0.94$; (a) mean, (b) turbulence intensity.

Since the hot-wire technique is inherently difficult and subject to question in compressible flows, the measurements are repeated at a low jet Mach number (0.3). Corresponding centerline variations of U and u' are shown in Fig. 12, in a similar manner as in Fig. 9. The trends appear essentially the same as seen in Fig. 9. This result encouraged further exploration at the lower Mach number with the expectation that the overall flow fields are also similar at the two Mach numbers. As stated in §2, detailed surveys could be carried out at the lower M_j with confidence and relative ease. An examination of the entire flow field was deemed important since centerline data for the asymmetric cases cannot fully represent the jet evolution.

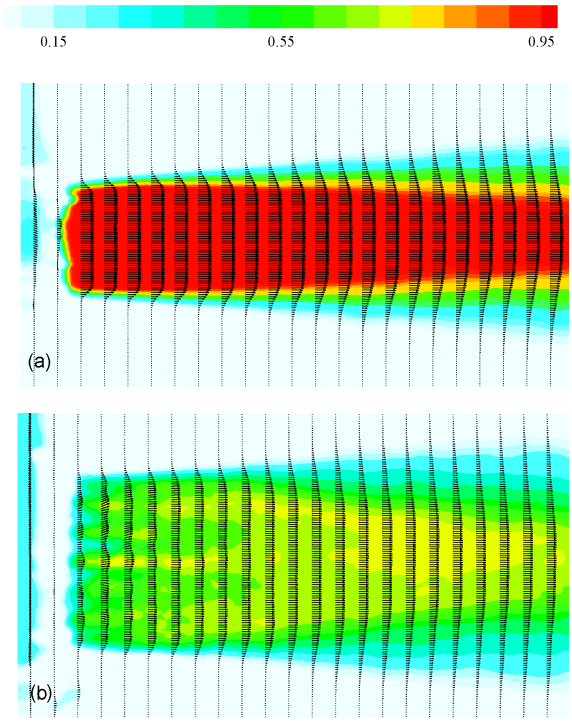

Figure 10. Mean velocity field on major-axis plane (DPIV data): (a) circular, (b) 14-lobed nozzles; $M_j \approx 0.94$.

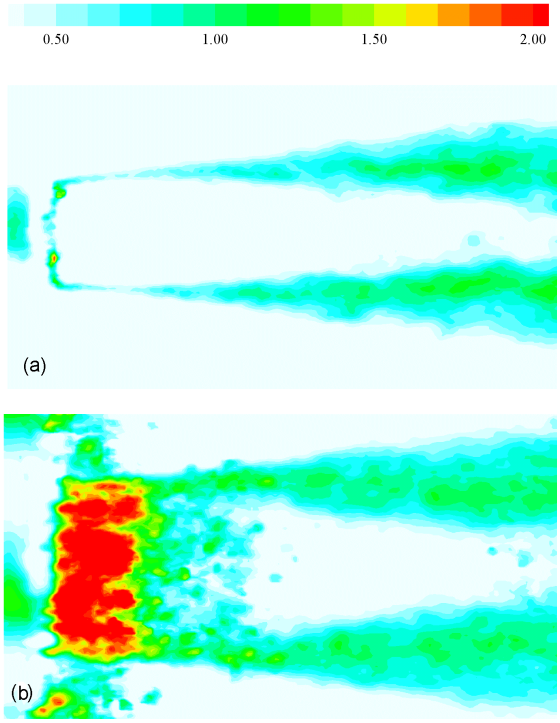

Figure 11. Turbulence intensity field on major-axis plane corresponding to the cases of Fig. 10.

First, surveys were conducted on a quadrant of the cross-section for only the 14-lobed nozzle. The surveys, involving as much as 36x20 grid points, were done at several x-stations. Mean velocity and turbulence intensity distributions are shown side-by-side, for several x/D, in Fig. 13. The 'cellular structure' in both U and u', due to the lobes, can be seen in the upstream regions. It becomes clear that the high turbulence intensity close to the nozzle occurs due to the shear layers shed from the lobes. The turbulence then decays—similarly as in the flow behind a turbulence-generating grid. Meanwhile, the turbulence is high in the outer shear layer that separates the jet from the ambient fluid. It is apparent that the second peak in the u'-profile for the lobed cases (Fig. 12) takes place following the merger of the outer shear layers.

If one assumes that the first peak occurs upon the merger of the shear layers shed from an individual lobe, it follows that the distance of the location of the first peak scales on the width of the lobes. Thus, the first peak should occur closer to the nozzle with smaller lobes. This is indeed the case in both Figs. 9 and 12. With reference to data of table 1, the first peak is found to occur in the *x/a* range of 4 to 6.

A complete description of the flow fields would require detailed data as in Fig. 13 over the entire cross-section at many x-stations. Carrying this out for all four nozzles was deemed formidable. Thus, in an attempt to compare and quantify the flow field evolution, only radial profiles were acquired at several x-stations covering the developing regions of the jets. The 10-lobed nozzle was excluded from this set of measurements, and data for the circular, 6- and 14-lobed cases were deemed sufficient. For the lobed cases, two profiles were obtained—one on the major axis and the other on the minor axis.

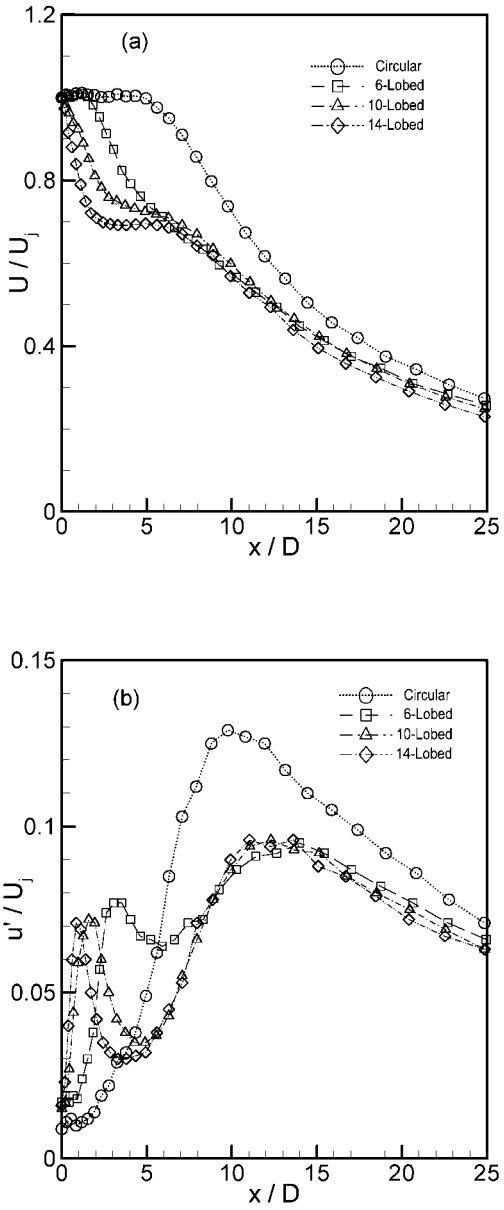

Figure 12. Centerline profiles at M_j = 0.30; (a) mean velocity, (b) turbulence intensity.

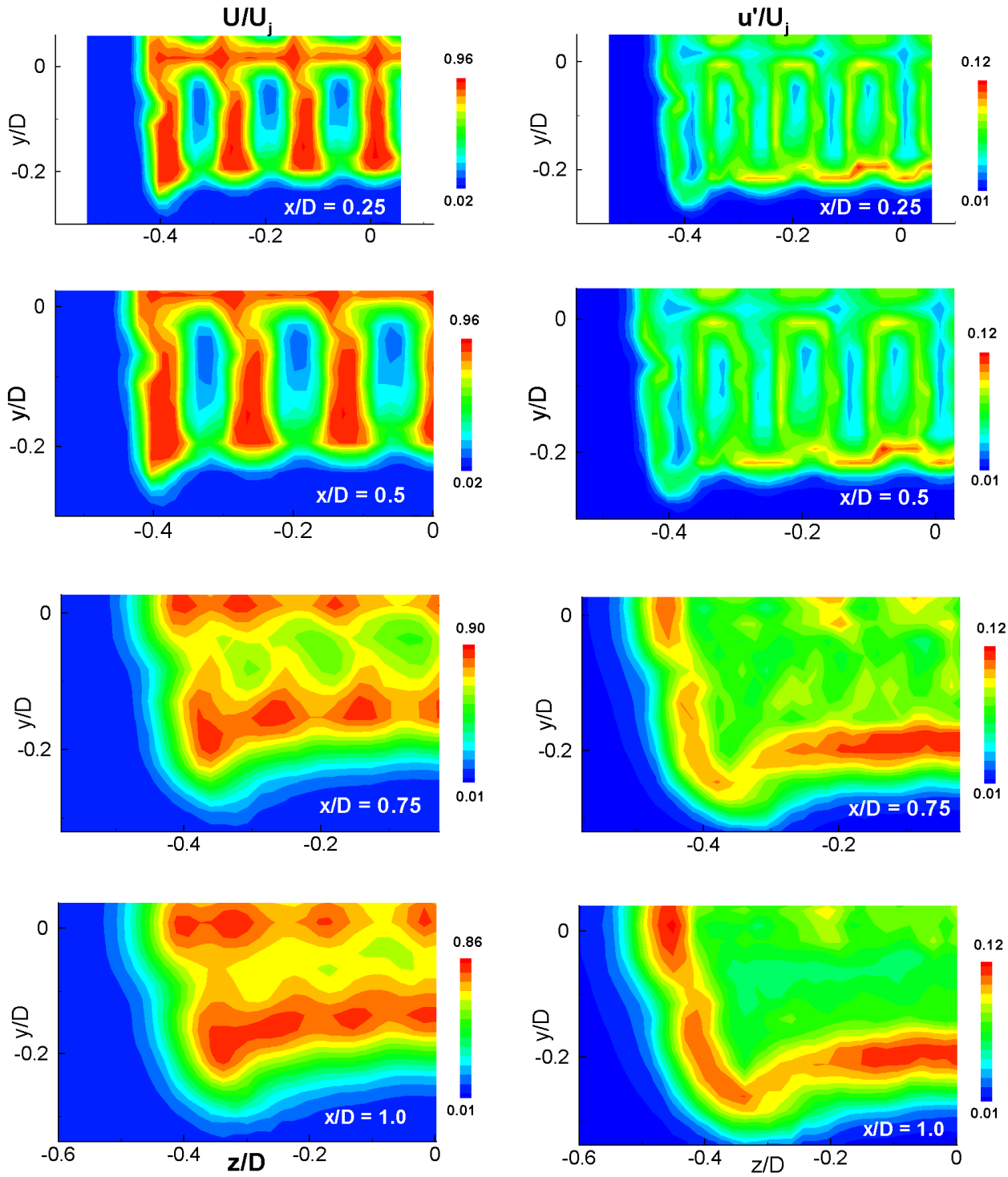

Figure 13. Cross-sectional distributions of mean velocity (left column) and turbulence intensity (right column) for the 14-lobed nozzle at indicated x/D locations; $M_j = 0.30$ (hot-wire data).

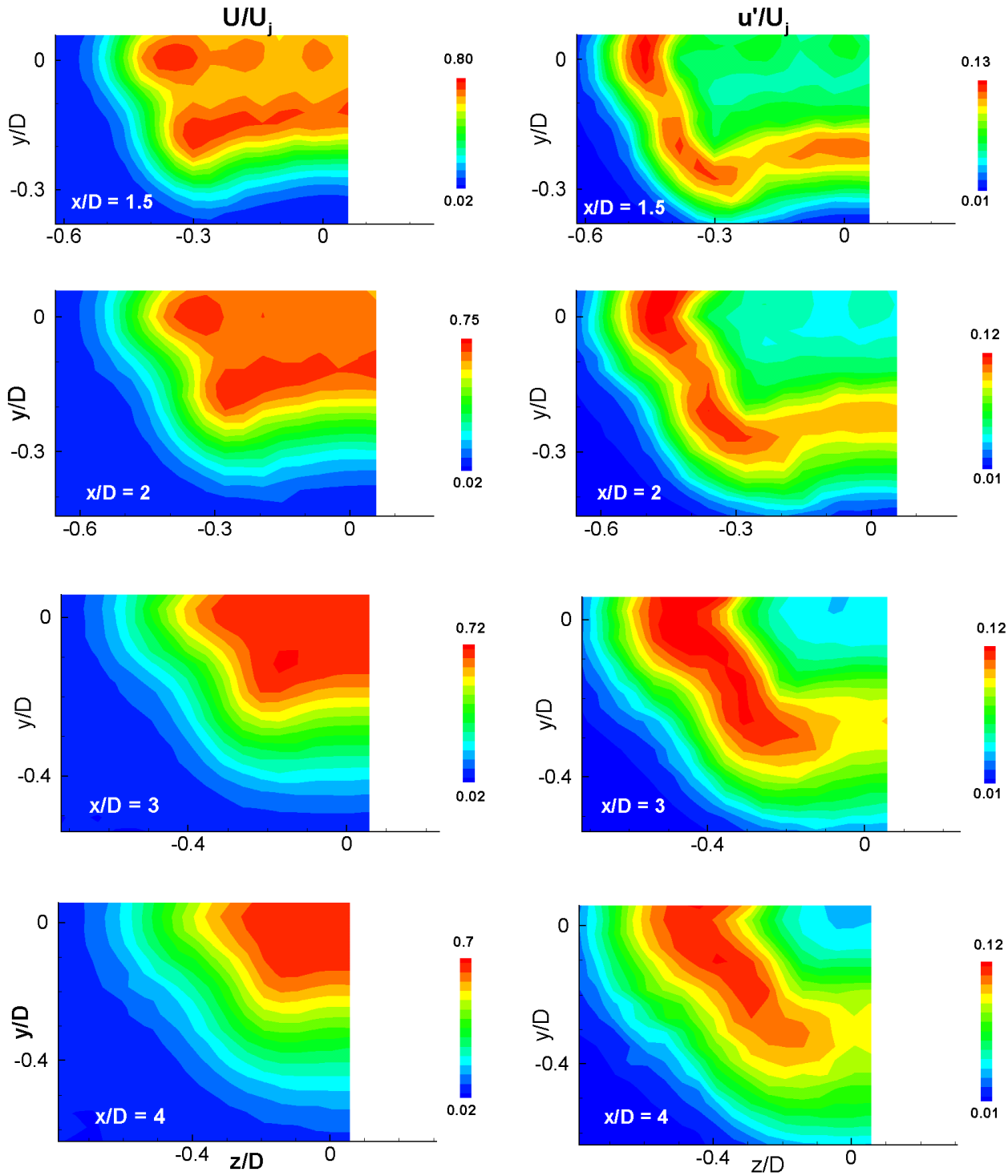

Figure 13 (concluded). Cross-sectional distributions of mean velocity (left column) and turbulence intensity (right column) for the 14-lobed nozzle at indicated x/D locations; $M_j = 0.30$ (hot-wire data).

The mean velocity profiles are compared in Fig. 14, while the corresponding turbulence intensity profiles are compared in Fig. 15. The flow field evolution until reaching the 'asymptotic state' can be gleaned from these data. The mean velocity profiles at the farthest x/D have become almost congruent (Fig. 14). However, the turbulence intensities are noticeably low for the lobed cases all across the jet. Close to the nozzle, an inspection of the data for the 14-lobed case reveals similarity between Figs. 10 and 14(a). The 'wavy' profiles match well. This agreement reinforces the notion that the 3-D flow fields at the low and high Mach numbers are essentially similar.

In order to compare the overall impact on the flow fields, the profiles of Figs. 14 and 15 were integrated. Two integrals, axial volume flow rate, $\dot{Q}$ and 'turbulent momentum flux', k^*, were calculated as follows:

$$\dot{Q}=2\pi\int rUdr, \qquad (1)$$

$$k^*=2\pi\int ru'^2dr, \qquad (2)$$

The integrals were normalized by the respective initial values, ($\dot{Q}_e$ =) A_eU_e and (K_e =) $A_eU_e^2$, where A_e is the area of the nozzle exit. The flow blockage for individual nozzles was taken into account in calculating A_e before data normalization.

For the circular jet, the integration was performed from the centerline in both positive and negative r-direction and an average of the two integrals was taken. For the lobed cases, similar averages were calculated on both major and minor axis planes. An average of the two averages was then taken for each case. It can be shown that such an average would be representative of the respective integral if the contours on the cross-sectional plane were elliptic in shape. This is a reasonable approximation for the lobed cases only after a distance of a few diameters from the exit. Thus, data close to the nozzle for the lobed cases are omitted in the following figures.

Streamwise variations of $\dot{Q}$ are shown in Fig. 16. The data for the circular nozzle may be compared with published results. The magnitudes and the slope (entrainment rate) agree reasonably with published data.[16] For either lobed case the magnitudes are higher indicating a faster jet spreading. However, the increase in $\dot{Q}$, say at *x/D* = 15, by about 20%, is rather modest. Mixing enhancement simply due to perimeter stretching has been inferred in Ref. 16 to be modest. Larger increases are reported in the cited reference when using other mixing enhancement techniques.

Those other techniques (e.g., vortex generators or periodic forcing at the 'preferred mode'), however, involve an increase in the turbulence intensities over most of the developing region of the jet. Here, the turbulence is high only close to the nozzle but subsequently it is remarkably low even as the jet evolves to reach the asymptotic state.

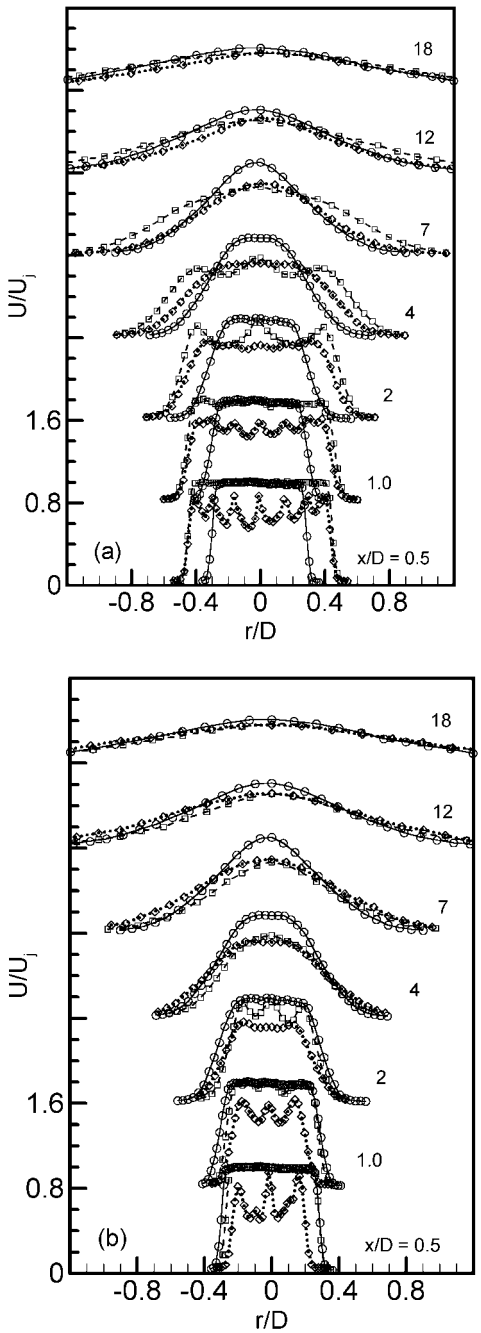

Figure 14. Cross-sectional profiles of axial mean velocity for circular (○), 6-lobe (□) and 14-lobe (◊) nozzles, M_j = 0.30: (a) major axis, (b) minor axis. Successive sets of profiles staggered by one major division.

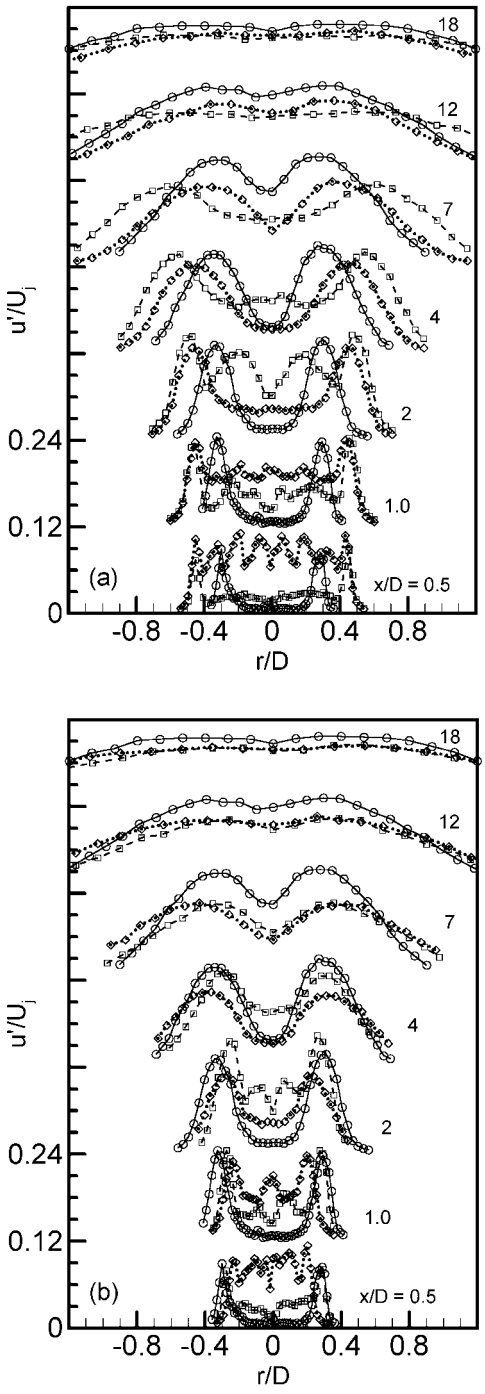

Figure 15. Turbulence intensity profiles corresponding to the data of Fig. 14: (a) major axis, (b) minor axis.

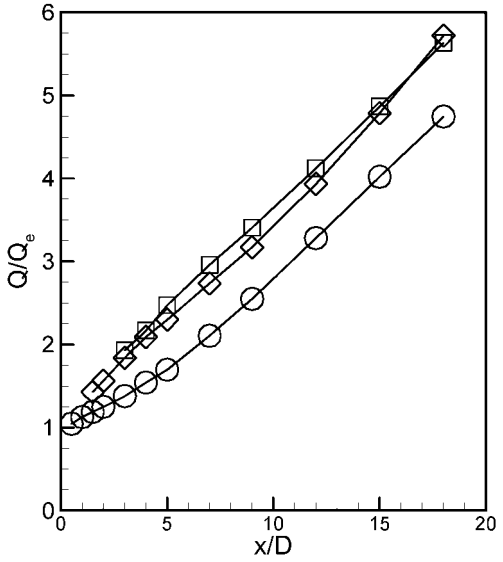

Figure 16. Axial volume flow rate versus x/D for circular (○), 6-lobe (□) and 14-lobe (◊) nozzles; $M_j = 0.30$.

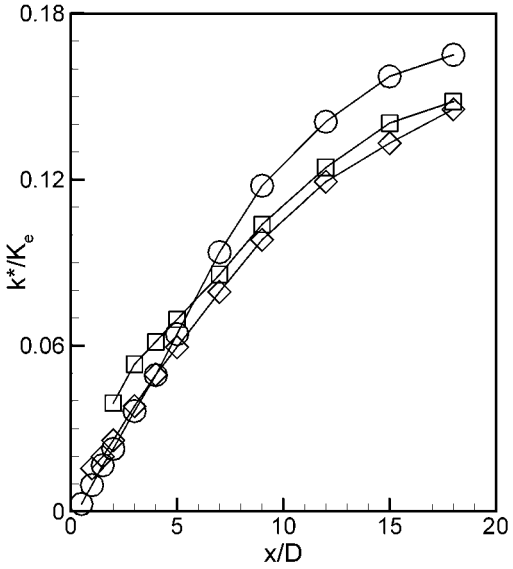

Figure 17. 'Turbulent momentum flux' versus x/D for circular (○), 6-lobe (□) and (◊), 14-lobe nozzles; $M_j = 0.30$.

Inspection of Fig. 15 reveals that while the turbulence for the lobed cases, say at x/D = 4, is low on the centerline it is high in the outer shear layer, compared to the circular case. Furthermore, these trends are different on the major and minor axis planes. Thus, a comparison based on the integral k^* is helpful and necessary to assess the overall impact. These data are shown in Fig. 17. It can be seen that for x/D > 6, the integrated turbulent kinetic energy k^* (turbulent momentum flux) is indeed consistently low for the lobed cases.

CONCLUDING REMARKS

Flow and noise fields of lobed nozzles are studied in this paper. The effect of number of lobes for a fixed exit area of the nozzle is considered.

All lobed nozzles involve a faster spreading of the jet compared to the circular case. On the centerline of the jet, the turbulence intensity exhibits a peak close to the nozzle followed by a second peak farther downstream. It is inferred that the first peak occurs when the shear layers from the lobes merge together. The distance of the location of the first peak, thus, scales as the width of the lobes. In comparison, the second peak occurs approximately eight jet diameters downstream. This occurs after the outer shear layers converge on the jet axis. The corresponding profile for the circular jet is characterized by only the second peak 8 to 10 diameters downstream. From somewhat downstream of the first peak, the turbulence intensities are significantly lower with the lobed nozzles compared to the circular case. This is true not only on the centerline but also reflects in the 'turbulent momentum flux' calculated by integration of the data over the cross section.

Increasing the number of lobes results in a progressive reduction in the turbulence intensities as well as overall noise. A reduction in noise is accompanied by a commensurate reduction in the turbulence intensity in the flow field. Increasing the number of lobes involves progressive reduction in the thrust coefficient. Among the cases studied, the six-lobed nozzle has the optimum reduction in turbulence and noise with minimal thrust penalty.

ACKNOWLEDGMENT

This work is supported by Aerospace Propulsion and Power Research and Technology Base Program at NASA Glenn.

REFERENCES

1. C.K.W. Tam and K.B.M.Q. Zaman, "Subsonic jet noise from nonaxisymmetric and tabbed nozzles," *AIAA J*., vol. 38, pp. 592–599, 2000.

2. K.B.M.Q. Zaman and C.K.W. Tam, "Flow and noise field of subsonic jets from asymmetric nozzles," *AIAA Paper* 99–3583, 30th AIAA Fluid Dynamics Conf., Norfolk, VA, June 1999.

3. J. Panda and K.B.M.Q. Zaman, "Density fluctuation in asymmetric nozzle plumes and correlation with far-field noise," *AIAA Paper* 2001–0378, 39th Aerospace Sciences Meeting, Reno, NV, January 2001.

4. D.C. McCormick and J.C. Bennett, "Vortical and turbulent structure of a lobed forced mixer free-shear layer," *AIAA J*., vol. 32, pp. 1852–1859, 1994.

5. S.C.M. Yu and T.H. Yip, "Measurements of velocities in the near field of a lobed forced mixer trailing edge," *The Aeronautical Journal*, March 1997.

6. M.A. Abolfadl, M.A. Metwally, A.M. El-Messiry, and M.A. Ali, "Experimental investigation of lobed mixer performance," *J. Prop. and Power*, vol. 17, Sept. 2001.

7. J.K. Elliott, T.A. Manning, Y.J. Qui, E.M. Greitzer, C.S. Tan, and T.G. Tillman, "Computational and experimental studies of flow in multi-lobed mixers," *AIAA Paper* 92–3568, 1998.

8. I.A. Waitz, E.M. Greitzer, and C.S. Tan, "Vortices in aero-propulsion systems," in *Fluid Vortices (ed. S.I. Green)*, pp. 471–532, Kluwer Academic Publishers, Netherlands, 1995.

9. E.K. Longmire, J.K. Eaton, and C.J. Elkins, "Control of jet structure by crow-shaped nozzles," *AIAA J*., vol. 30, p. 505, 1992.

10. J. Lasheras and K. Prestridge, "Three-dimensional vorticity dynamics in coflowing jets subjected to axial and azimuthal forcing," *AIAA Paper* 97–1880, 28th AIAA Fluid Dynamics Conf., Snowmass, CO, June 27–July 2, 1997.

11. M. Samimy, J.-H. Kim, P.S. Clancy and S. Martens, "Passive control of supersonic rectangular jets via nozzle trailing-edge modifications," *AIAA J*., vol. 36, p. 1230, 1998.

12. J.-H. Kim and M. Samimy, "Mixing enhancement via nozzle trailing edge modifications in a high speed rectangular jet," *Physics of Fluids*, vol. 11, September 1999.

13. M.M. Gilinsky and J.M. Seiner, "Corrugated nozzles for acoustic and thrust benefits," *AIAA Paper* 96–1670, 2nd AIAA/CEAS Aeroacoustics Conference, State College, PA, May 6–8, 1996.

14. H. Hui, T. Kobayashi, T. Saga, N. Taniguchi, H. Liu and S. Wu, "Research on the rectangular lobed exhaust ejector/mixer systems," *Trans. Japan Soc. Aer. Space Sci*., Feb. 1999.

15. H. Hu, T. Kobayashi, T. Saga, S. Segawa, and N. Taniguchi, "Particle image velocimetry and planar laser-induced fluorescence measurements on lobed jet mixing flows," *Experiments in Fluids*, Supplemental Issue, S141–157, Springer-Verlag, 2000.

16. K.B.M.Q. Zaman, "Spreading characteristics of compressible jets from nozzles of various geometries," *J. Fluid Mech.,* vol. 383, pp. 197–228, 1999.

17. F. Scarano and M.L. Riethmuller, "Advances in iterative Multigrid PIV Image Processing," *Experiments in Fluids*, Supplemental Issue, S51–60, 2000.